

## THE PHYSICS PROBLEM OF THE SPALLATION NEUTRON PRODUCTION SOURCE RELATED TO ACCELERATOR-DRIVEN SYSTEMS

**Sheng Fan,<sup>1</sup> Hongzhou Zhang,<sup>1,2</sup> Yanlin Ye<sup>3</sup> and Zhixiang Zhao<sup>1</sup>**

1. China Institute of Atomic Energy, Beijing 102413, China

2. Physics Department, Northwest University, Xi'an 710069, China

3. Physics College, Peking University, Beijing 100871, China

### Abstract

In present work, the SHIELD code system have been used to investigate the physics properties of spallation neutron target, such as the neutron spectra, the yield, the radioactivity in the target and the target size etc. The fragment mass distribution of the residual nuclei from proton-induced spallation reaction on thick lead target with energy 1.6 GeV have been analysed also. Radiation damage, such as radiation damage cross-section, displacement atom cross-section, the rate of displacement atom, and displacement production rates in target Pb induced from intermediate energy proton and neutron incident were investigated.

## Introduction

ADS system consists of three parts: accelerator, spallation neutron target and sub-critical reactor. The spallation neutron source induced by intermediate energy proton-nucleus interaction is an important link for transmutation and applications. [1-3]

In this work, we use the SHIELD [4-6] code to simulate the physics properties of the spallation neutron target proton-induced. The SHIELD calculations have been compared with experimental data, such as the neutron spectra, the radioactivity in the target and the target size. The geometric design and the visualisation performances are largely improved by inserting the relevant package of the GEANT into the SHIELD. [7] The pair correction, the parameters of the level density related with energy and the time scale of the charge of reaction mechanism in the process of reaction studied at Reference [8-11] are introduced into the SHIELD code to study fragment distribution and excitation function of the residual nuclides proton-induced with intermediate energy.

The fragment mass distribution and excitation function of the residual nuclei from proton-induced spallation reaction on thin Pb target with intermediate energy have been analysed. And the results are in good agreement with measured data. The fragment mass distribution of the residual nuclei from proton-induced spallation reaction on thick Pb target with energy 1.6 GeV have been analysed also. Radiation damage, such as radiation damage cross-section, displacement atom cross-section, the rate of displacement atom, the gas production cross-section, the rate of gas production and the ratio, R, of the helium and displacement production rates in target, container window and spallation neutron source materials: W, Pb induced from intermediate energy proton and neutron incident were investigated. And the study of radiation damage in the thick Pb target with length 60 cm, radius 10 cm was completed and the map of the displacement atom in all target was obtained. In the mean time, the energy deposit in the target of  $^{208}\text{Pb}$  with the length 60 m and the radius 10 cm proton-induced is analysed. The results calculated by SHIELD code are in good agreement with the measured data of 1 GeV proton into the Be, C, Al, Cu, Pb and depleted U targets. [12] The maps of power density distribution in the target are obtained with the proton beam intensity 10mA and the energy 1.5 GeV.

## Calculations

Figure 1 gives the prediction of SHIELD on the energy spectra of neutrons for incident proton energy of 150(a) and 1 500 MeV(b) bombing on the thick lead target with the length of 60 cm and radius of 10 cm, respectively. It is clear that the neutron spectra are much softer at 150 MeV than 1 500 MeV. However, even at 1 500 MeV beam energy, most neutrons escaped from the thick target are concentrated at energies below about 20 MeV, which could also be generated by the research facility of 150 MeV linac.

Figure 2 shows the mass distribution of the residual nuclear fragments induced by pencil proton bombarding the thick Pb target of the length 60 cm and and the radius 20 cm with the incident energy 1.6 GeV. It is clear that all products of the residual nuclides are located at the vicinity of the target.

Figure 3 is shown the calculated radioactivity of a cylindrical Pb target, which is radiated by a pencil beam of 30 mA intensity for 1 year. The proton beam energy for Figure A and Figure B are 150 MeV and 1 500 MeV, respectively. They show the time dependence of radioactivity caused by proton, neutrons and low energy ( $E_n \leq 14.5$  MeV) neutrons. From Figure 3(B), It is found that the activity is mainly caused by higher energy ( $E_n \geq 14.5$  MeV) neutrons. From Figure 3(A), It is noticeable that at 150 MeV the radioactivity is mainly caused by proton, which is in contrast to the case at 1 500 MeV. This means that under the irradiation of 150 MeV protons, the proton reaction data is more important than the neutron's is the study of target property.



In order to investigate the radiation damage of the all thick target for ADS system, we divided the cylinder lead target with length 30 cm and radius 10 cm into 100 parts. The each part is 3 cm on the length and  $R_i$  on the radial axis, the radius,  $R_i$  are suffered from,

$$\begin{aligned} R_1^2 &= R_2^2 - R_1^2 \\ &= R_3^2 - R_2^2 \\ &= R_{10}^2 - R_9^2 \end{aligned}$$

Figure 4. The radiation damage cross-section on Z axis proton induced into target with incident energy 1.5 GeV

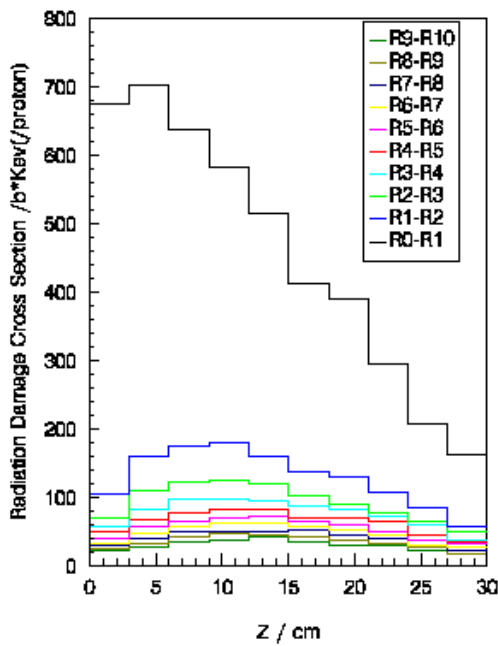


Figure 5. The radiation damage cross-section on R axis proton induced into target with incident energy 1.5 GeV

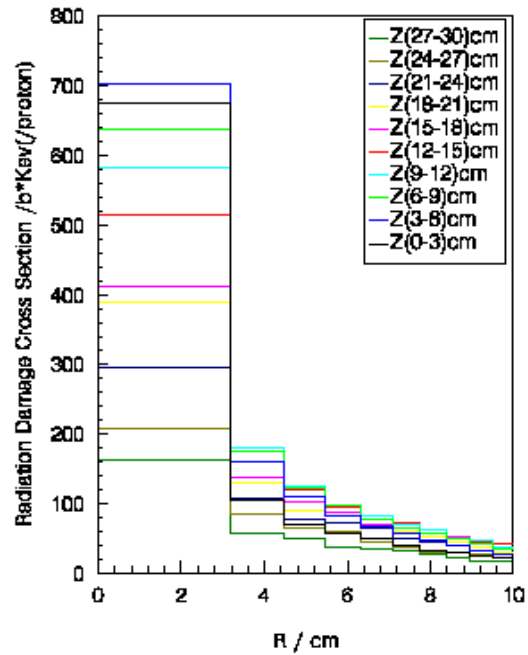


Figure 4 gives the radiation damage cross-section per proton distribution on Z axis in the lead target of 30 length and 10 cm radius with the pencil proton beam energy 1.5 GeV. It is clear that the radiation damage cross-section decrease when the Z values increase, and while the  $R_i$  increase, it increase also.

Figure 5 shows the same as Figure 4, but on the R axis. We found that the radiation damage cross-section in the incident point is not the largest value in the target, but there is largest value at the area of the Z (3~6 cm) in all the target, and while the R increase the location of the largest value is increasing. The reason is that the contribution of the low energy neutrons is important, and in the incident point, the number of the low energy neutron is much less than that of the area at Z (3~6 cm) on the centre area.

In the present work, we analyse the energy deposit in the lead cylinder target of 60 cm in length and 10 cm in radius proton-induced with the energy 1.5 GeV and the current 10 mA. The energy deposit mainly consists of energy loss of ionisation, the recoil energy of the residual nuclide and the energy of the fission fragment. In order to study the detailed distribution of the energy deposit in the target, the cylinder lead target is divided into 300 parts which the mass and the volume of each part is equal, there are 30 parts on the length and each parts on the length is 2.0 cm.

Figure 6. The power density distribution on Z axis

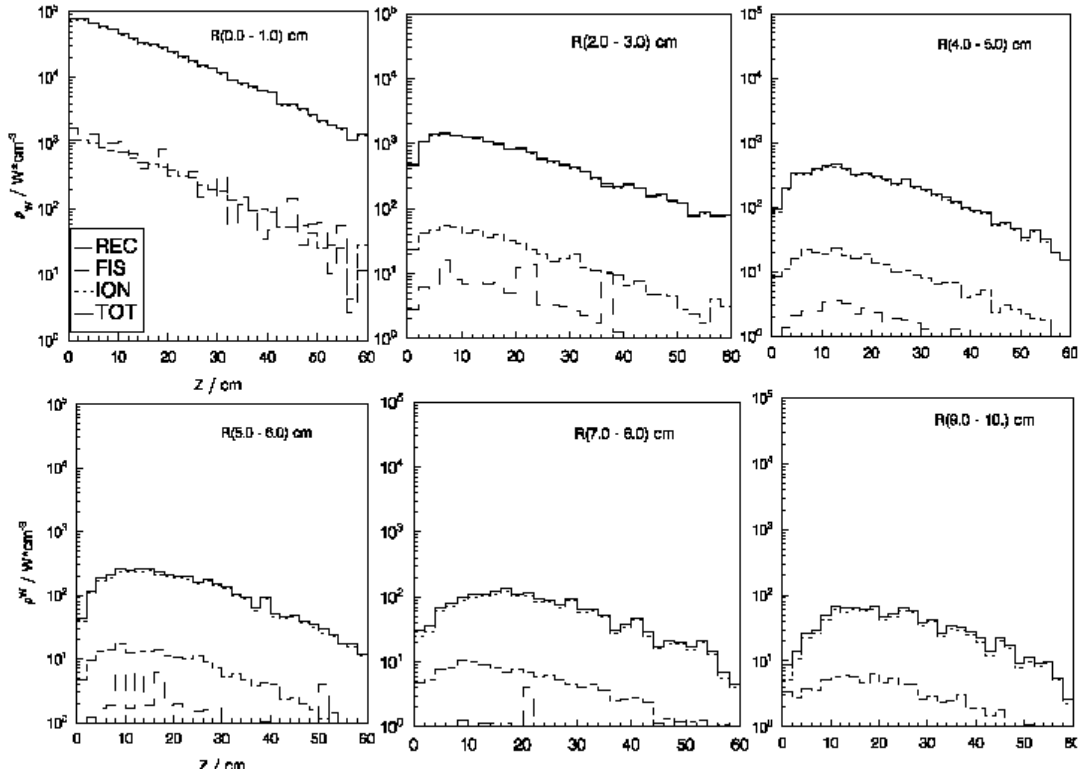


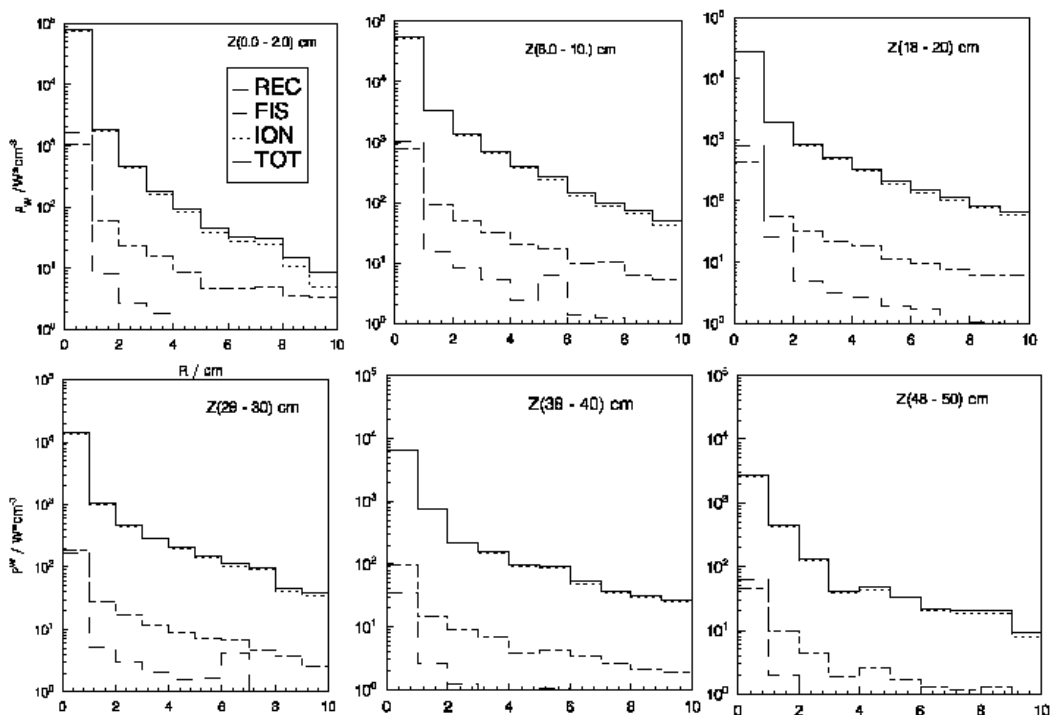
Figure 6 and 7 give the distribution of the energy deposit on Z and R axes for the lead target with the length of 60 cm and radius of 10 cm proton-induced with the energy 1.5 GeV and the current 10 mA. From Figure 6 and 7, they are clear that the contribution of the ionisation loss energy is the largest and the fission fragment energy is lowest. We also found the power density at incident point ( $Z=0$ , and  $R=0$ ) is largest in all the target, and it decrease on the Z axis while Z increase, and while the R increase, we found there is a largest value in the power density distribution, and the location of the largest value in the target increase on the Z axis, because the contribution of the cascade-charge particle in the area have a larger fraction in the total power density.

### Summary and discussions

In this work, we analyse the properties of the spallation neutron source, such as the neutron energy spectra, the residual nuclear mass distribution and the radioactivity in the target, the radiation damage and the energy deposit proton-induced with intermediate energy by using improved SHIELD code system.

We can find that the neutron spectra are much softer at 150 MeV than 1 500 MeV. However, even at 1 500 MeV beam energy, most neutrons escaped from the thick target are concentrated at energies below about 20 MeV, which could also be generated by the research facility of 150 MeV linac. For the mass distribution, all products of the residual nuclides are located at the vicinity of the target. The activity is mainly caused by higher energy ( $E_n \geq 14.5$  MeV) neutrons with the incident proton energy of 1 500 MeV. However, it is noticeable that at 150 MeV the radioactivity is mainly caused by proton, which is in contrast to the case at 1 500 MeV. This means that under the irradiation of 150 MeV protons, the proton reaction data is more important than the neutron's is the study of target property. We found that the contribution of the ionisation loss energy is the largest and the fission fragment energy is lowest.

Figure 7. The power density distribution of the radial axis



## REFERENCES

- [1] C.D. Bowman, E.D. Arthur, P.W. Lisowski *et al.* (1992), *Nuclear Energy Generation and Waste Transmutation using an Accelerator-driven Intense Thermal Neutron Source*, Nucl. Instr. and Meth. A320, 336~367.
- [2] F. Carminati, R. Klapisch, J.P. Revol *et al.* (1993), *An Energy Amplifier for Cleaner and Inexhaustible Nuclear Energy Production Driven by a Particle Accelerator*, CERN/AT/93-47(ET) Report.
- [3] C. Rubbia, J.A. Rubio, S. Buono *et al.* (1995), *Conceptual Design of a Fast Neutron Operated High Power Energy Amplifier*, CERN/AT/95-44(ET), Report.
- [4] A.V. Dmentyev, N.M. Sobolevsky (1997), *SHIELD – Universal Monte Carlo Hadron Transport Code Scope and Application*, Proc. of 3<sup>rd</sup> Workshop on Simulating Accelerator Radiation Environments, May 7-9.
- [5] KEK, Tsukuba, N.M. Sobolevsky (1995), *Conclusions of International Code Comparison for Intermediate Energy Nuclear Data*, NSC/DOC(95)2.
- [6] S.F. Sidorkin, A.V. Dmentyev, N.M. Sobolevsky *et al.* (1996), *Pulsed Neutron Source on the Basis of a Uranium Target at the Moscow Meson Factory*, Nucl. Instr. And Meth., A370, 467-476.
- [7] Xu Chuncheng, Ye Yanlin, Chen Tao *et al.*, *The Target Practical Design for ADS Using SHIELD Code*, High Energy Physics and Nuclear Physics, 23(12), 673~677, (in Chinese).
- [8] Fan Sheng, Li Zhuxia Zhao Zhixiang *et al.* (1999), *Analysis of Proton-induced Reactions on <sup>208</sup>Pb with Incident Energy 590 MeV and 322 MeV*, Eur. Phys.J.A4, 61-69.

- [9] Fan Sheng (1998), *Two Physical Problems Related to Accelerator-driven Radioactive Clean Nuclear Power System*, Ph.D. thesis, China Institute of Atomic Energy, Beijing, China.
- [10] S.G. Mashnik, A.J. Sierk, O. Bersillon *et al.* (1998), *Cascade-exciton Model Developed Analysis of the Protonspallation at Energies from 10 MeV to 5 GeV*, Report LANL.
- [11] Fan Sheng, Rong Jiang *et al.*, *The Mass Distribution of Nb, Au and Pb Induced Reactions from Proton Incident with Energies Range from 100 MeV to 3 GeV*, submitted to Nucl. Sci. and Eng.
- [12] V.I. Belyakov-Bodin, V.D. Kazaritsky, A.L. Povarov *et al.* (1990), *Calorimetric Measurements and Monte Carlo Analysis of the Medium-energy Protons Bombarding Lead and Bismuth Targets* [J]. Nucl Instr Meth, A295:140-146.